Flow Measurement and Instrumentation 33 (2013) 239–243

Contents lists available at ScienceDirect

Flow Measurement and Instrumentation

journal homepage: www.elsevier.com/locate/flowmeasinst

Three-dimensional MHD simulations of the electromagnetic flowmeter for laminar and turbulent flows

Bo Lu [a,*], Liangwang Xu [b], Xiaozhang Zhang [c]

[a] Institute of Plasma Physics, Chinese Academy of Sciences, Hefei, Anhui 230031, China
[b] Shanghai Branch, China Nuclear Power Technology Research Institute, Shanghai 200030, China
[c] Department of Engineering Physics, Tsinghua University, Beijing 100084, China

ARTICLE INFO

Article history:
Received 25 November 2012
Received in revised form
10 April 2013
Accepted 26 July 2013
Available online 14 August 2013

Keywords:
Electromagnetic flowmeter
CFD simulation
Lorentz force
Induced electric field
Turbulent flow

ABSTRACT

The interaction between an electrically conducting fluid and an external magnetic field in an ideal cylindrical electromagnetic flowmeter is numerically investigated for both laminar and turbulent flows. Induced electric potential in the fluid, and the difference in potential at the measuring electrodes are directly obtained by including MHD effects in the CFD simulations. Fully developed laminar and turbulent flows are simulated. The computed electric potential difference on the electrodes agrees with analytical values for small Hartmann number cases, where the induced Lorentz force is small. Turbulent flow produces a more uniform electric potential distribution in the flow meter cross-section than laminar flow. These integrated MHD/CFD simulations couple the MHD effect with flow dynamics without deriving a weighting function with an assumed velocity profile, which will be necessary for electromagnetic flow meters when the Hartmann number is not small.

1. Introduction

The analysis and characterization of an electromagnetic flowmeter output signal normally involves numerical evaluation of a weight function using pre-known or assumed velocity profiles, where the weight function is derived analytically as *a priori*. The electric potential difference between two electrodes on opposite sides of the pipe is then established as a function of the flow rate.

Shercliff [1] derived the weight function applicable for rectilinear flows in an electromagnetic (EM) flow meter. This approach was widely adopted hitherto in predicting the output signal of EM flowmeters. He showed that the output signal for a circular flowmeter was independent of the velocity profile for axisymmetric flows. He established the first thorough theoretical approach for understanding the characteristics of EM flowmeters [2]. Bevir [3] further explored the weight function method (WFM) in three dimensions, in which he introduced a weight vector $\boldsymbol{W}$ and laid out the design requirements on $\boldsymbol{W}$ for an ideal flowmeter whose output signal was not dependent on the velocity profile, but only on the flow rate. The weight function method has since been applied in-depth to characterize EM flowmeters in terms of realistic magnetic field data and flow profile sensitivity for various electrode shapes [4–6].

Analytical solution of the governing equations was also proposed by Nashed [7] for non-uniform magnetic induction and axisymmetric velocity and conductivity profiles using a power series method. To accommodate various magnetic and electrode configurations, Hemp and Versteeg [8] started from the magnetic potential and virtual current potential using Fourier series expansion for a finite fluid volume and derived a weight function that was also represented by a Fourier series. Luntta and Halttunen [9] studied the effects of velocity profiles including a parabolic laminar flow and a turbulent flow using an empirical correlation and concluded that the flowmeters were sensitive to disturbances in the flow, suggesting that accurate flow modeling was important.

More recently, numerical studies of the EM flowmeter were undertaken to overcome the limitations of analytical methods in addressing complex geometries and flow conditions. Zhang and Hemp [10] proposed a semi-analytical method for calculating the virtual current using an alternating Schwartz scheme for certain boundary conditions. Numerical solutions of the governing equations for electric potential were also obtained directly using finite volume method and finite element method. Lim and Chung [11] used the finite volume method and compared the results with the weight function method for laminar and turbulent velocity profiles. Generally good agreement was achieved, but distortion was present and outcomes were sensitive to the numerical grids. They also investigated the installation effects for a 90° elbow that created strong asymmetric flow, and concluded that the disturbance in the flow strongly affected the signal [12]. Wang, Lucas

* Corresponding author. Tel.: +86 55165591309; fax: +86 55165591310.
E-mail address: blu@ipp.ac.cn (B. Lu).

0955-5986/$ - see front matter © 2013 Elsevier Ltd. All rights reserved.
http://dx.doi.org/10.1016/j.flowmeasinst.2013.07.015

and Tian numerically evaluated the weight function using finite element method in COSMOL© using a 'fluid pixel' method and the results agreed well with the theoretically method [13]. They further applied this method towards the relationship between the velocity profiles and flowmeter signals for two-phase flows [14]. Numerical methods have been shown to be a very powerful tool in predicting the characteristics of an EM flowmeter, for which complex geometries and magnetic field can be accounted for. In those studies the velocity field is first obtained and used as input for the calculation of the weight function or induced electric potential. On the other hand, integrated MHD/CFD simulations have been widely applied to liquid–metal flow subjected to magnetic field, such as in the Lorentz force flowmeter [15]. Integrated MHD/CFD simulations are also employed in fusion reactor design [16], where the electromotive force influence on the flow cannot be ignored.

The electromagnetic flowmeter is within the scope of magnetohydrodynamics (MHD), in which the flowing conducting fluid interacts with the magnetic field and generates an induced magnetic and electric field. The induced current and magnetic field also result in a Lorentz force, which should be represented as a momentum source in the momentum equation. The induced Lorentz force, if strong enough, may affect the velocity profile [17]. The widely applied weight function method uses a prescribed velocity profile as the input when evaluating the output signal of an electromagnetic flowmeter. The weight function method tacitly assumes the velocity profile is unchanged in the presence of a magnetic field, and should only be used when the Lorentz forces can be ignored.

Following Moreau [18], the MHD model adds an induction equation to the regular fluid dynamic equations to include the interaction between the velocity field and the magnetic field,

$$\frac{\partial \vec{B}}{\partial t}+(\vec{V}\times\nabla)\vec{B}=\frac{1}{\mu\sigma}\nabla^2\vec{B}+(\vec{B}\times\nabla)\vec{V} \tag{1}$$

where $\vec{B}$ is the external and induced magnetic field; $\vec{V}$ is the velocity vector; μ and σ are permeability and electric conductivity, respectively.

The induced current ($\vec{j}$) is related to the magnetic field and generates the Lorentz force ($\vec{F}_L$) that tends to oppose the flow direction,

$$\vec{j}=\frac{1}{\mu}\nabla\times\vec{B} \tag{2}$$

$$\vec{F}_L=\vec{j}\times\vec{B} \tag{3}$$

Combined with the conventional fluid dynamics equations, the induced magnetic field, electric field, current density, electric potential can be solved simultaneously. The dimensionless Hartmann number (Ha) is normally used to characterize the ratio of electromagnetic force to the viscous force in magnetohydrodynamics

$$Ha=BL\sqrt{\sigma/\mu} \tag{4}$$

where L is the characteristic length of the MHD model.

For EM flowmeters, Ha should be as small as possible, such that the velocity field is not altered significantly by the induced electromagnetic force. This is often true for liquids with small electric conductivity, however, for liquid metals, Ha may be much bigger than 1.0 and the electromagnetic force cannot be ignored.

The current study numerically simulates behaviors of an electromagnetic flowmeter. Typical laminar and turbulent flow conditions are simulated to obtain the topology of induced current and electric potential. The studies were performed using the FLUENT© code, in which the MHD module was invoked for integrated MHD/CFD simulations. Section 2 presents the CFD model used for simulations. Detailed simulation results for both laminar and turbulent flow conditions are summarized and discussed in Section 3. Conclusions are given in Section 4.

2. Modeling of a electromagnetic flowmeter

A cylindrical electromagnetic flowmeter model was developed as shown in Fig. 1 with the flowmeter radius set at $R=0.01$ m. It includes three sections: inlet section ($L_1=\pi R$), measurement/induction section ($L_2=2\pi R$) and outlet section ($L_3=\pi R$). A uniform magnetic field predominately in the y direction was applied only in the induction section. The wall of the flowmeter is assumed to be electrically insulated. The length of induction section is chosen so that nearly all the contribution from the flow to the induced electric potential is included in the output signal, measured through two point electrodes located on two opposite positions with spacing equal to the flowmeter diameter [3]. Conducting fluid enters from the left and passes through the induction zone before exiting the flowmeter.

The flow is assumed to be fully developed at the inlet, with velocity magnitude only a function of radial position. In the flow direction (x coordinate), uniform discretization was applied, while in the traverse direction, a structured mesh was created in GAMBIT© as shown in Fig. 2. A boundary layer was created at the wall to improve the resolution near the wall where gradients may be steep. At the center, a much coarser discretization scheme was adopted since the velocity gradient is much smaller. Several meshes with different numbers of cells were used to establish grid sensitivity and convergence.

Laminar and turbulent flow conditions were used to study the characteristics of the induced electric potential in the flowmeter. A parabolic velocity profile with average velocity of 0.1 m/s ($Re=1992$) was imposed at the flowmeter inlet as an inlet condition for the MHD/CFD solution,

$$V(r)=V_0(1-(r/R)^2) \tag{5}$$

where $V(r)$ is the axial velocity at the radius r, V_0 is the average velocity and R is the radius of the pipe.

For the turbulent flow case, the imposed inlet velocity profile approximately follows the exponential form with an average velocity of 1.0 m/s ($Re=19{,}920$),

$$V(r)=V_{\max}(1-(r/R))^{1/n} \tag{6}$$

where $V(r)$ is the axial velocity at the radius r; $V_{\max}$ is the maximum velocity at $r=0$; R is the radius of the pipe and the exponent $1/n$ is determined empirically as a function of Reynolds number,

$$n=1.66\log(Re) \tag{7}$$

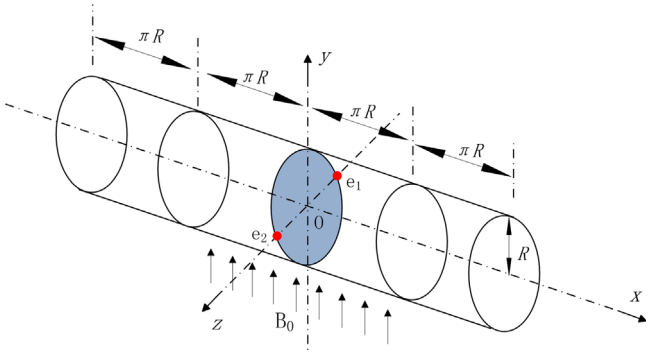

Fig. 1. Schematic of a cylindrical electromagnetic flowmeter model. (Flow is in the positive x-direction; B_0 is applied in the positive y-direction and over a length of $2\pi R$; two electrodes are located on the inner surface in the x–z plane).

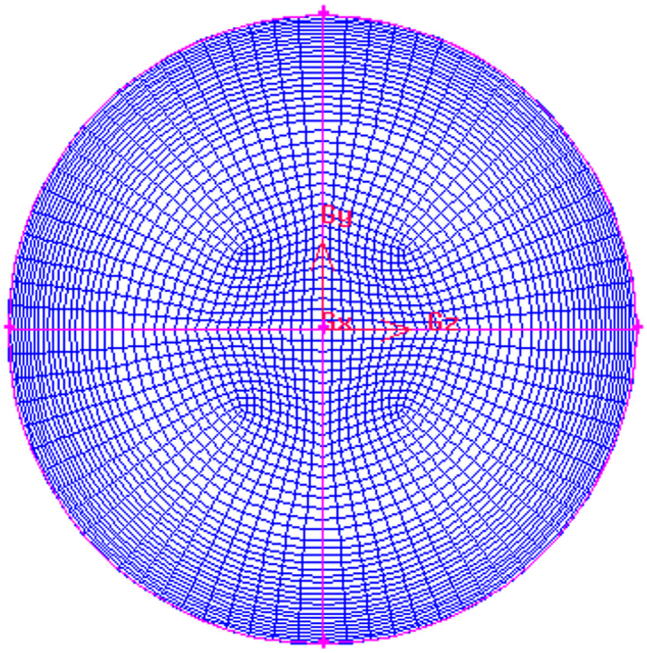

Fig. 2. Grid structure in the flowmeter's cross section.

Table 1
Physical properties and constants used in the simulations.

Density (kg/m^3)	Dynamic viscosity (kg/m-s)	Electric conductance (S/m)	Magnetic permeability (h/m)	B_0(T)	V_0 (m/s)	
					Laminar	Turbulent
998	0.001	0.01	1.26e-6	0.1	0.1	1.0

The exponential inlet turbulent velocity profile is only an approximate empirical correlation. The actual velocity profile along the flow direction is different even this imposed inlet profile. To handle this, a uniform velocity profile is first applied at the inlet to obtain a velocity profile at the exit. This exit profile is then used as the inlet boundary condition to generate another velocity profile at exit. This process was repeated until a fully developed velocity profile is achieved along the flow direction. This final velocity profile is then saved and used at the inlet condition for turbulent MHD simulations.

3. CFD simulation results and discussions

This section summarizes the detailed simulation results for both laminar and turbulent flows. Before switching on the magnetic field, simulations were performed to study the grid dependence. After a suitable grid with good accuracy was established, MHD simulations were performed to study the characteristics of the flowmeter under different flow conditions. For turbulent flow, a standard k–ε model with standard wall functions was used. In all the simulations, material properties and relevant constants in Table 1 were applied. For numerical schemes, second-order differencing was applied for the momentum, continuity and the magnetic equations, all of which are iterated till the relative change in the variables fall below 1.0×10^{-6}.

3.1. Grid independence study

To minimize the effect of different model discretization schemes on the simulation results, it is necessary to carry out simulations at different grid sizes to ensure the results are nearly independent of the grid size.

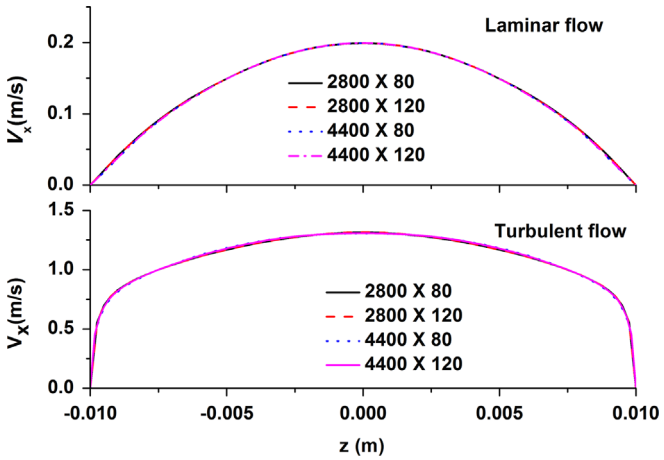

Fig. 3. Velocity profiles under different grid densities.

Four different grid discretization schemes were tested. N_x is the number of nodes in the x direction and N_{yz} is the grid number in the y–z cross section. Grids with N_x=2800 or 4200 and N_{yz}=80 or 120 were tested. Fig. 3 shows the x-component velocity profiles along the chord connecting the electrodes (z direction) for both laminar and turbulent flow at various grid densities.

It can be seen that the simulation results were very similar at different grid densities. Also noted is the much broader velocity profile obtained in the turbulent case. Based on the simulations, grid structure with 2800×80 was used in the following MHD simulations for both good resolution and simulation efficiency.

3.2. Simulation results for laminar flow

In the laminar flow case, a uniform magnetic field in the y direction (B_0=0.1 T) is applied in the induction section. The fully developed rectilinear velocity profile was imposed at the inlet with an average velocity of 0.1 m/s. Initially, to be consistent with assumption used in the electromagnetic flowmeter, the Lorentz force is not invoked and the induced magnetic field is solved independently with respect to the velocity field. Fig. 4 shows the distribution of x-component velocity (V_x), z-component electric (E_z), z-component current density (j_z) and induced electric potential (U) along the chord connecting two electrodes. It can be seen that the parabolic velocity profile also results in a parabolic electric field. The electric field and current density reach maximum at the center of the flowmeter where the velocity is maximum. The electric potential increases gradually between the electrodes and changes sign across the flowmeter axis. The electric potential at the axis is chosen to be zero and used as the reference point. The difference in electric potential at the electrodes is about 0.2 mV, which corresponds to the theoretical value for axisymmetric velocity and a uniform magnetic field as follows,

$$\Delta U = B_0 V_0 2R \tag{8}$$

The simulations reproduce the electric potential predicted through the analytical method. The detailed contour of electric potential on the vertical cross section passing through the electrodes was also shown in Fig. 5. It shows a symmetric distribution of the magnitude. Maximum difference is achieved where electrodes are located on the end points of the transverse chord with length equal to the diameter.

The effect of induced Lorentz force on the velocity profile, and consequently the electric potential, was examined by including the Lorentz force in the momentum equation. For this case, the Hartmann

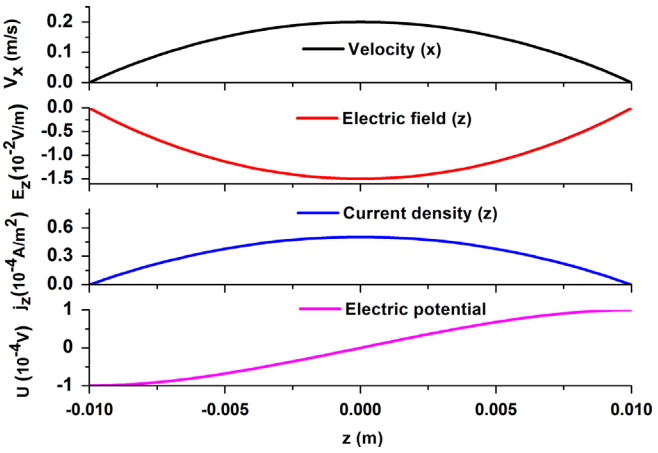

Fig. 4. Profile of velocity, electric field, current density and electric potential along the chord connecting the electrodes for a laminar flow.

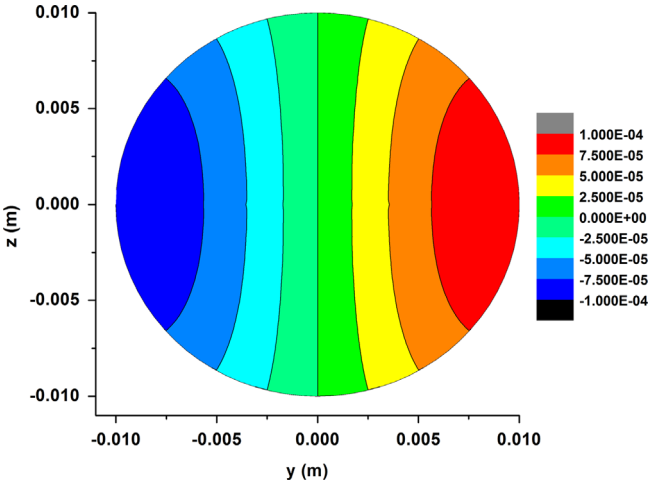

Fig. 5. Contour of electric potential in the vertical cross section of flowmeter pass the electrodes.

number was evaluated and equal to 0.0063. Since it is very small, it was expected that the velocity profile would not be affected substantially by the Lorentz force.

Fig. 6 shows the velocity profile and electric potential distribution with Lorentz force on and off, respectively. There was no appreciable change in the velocity field or the induced electric potential due to the very small magnitude of electromagnetic force.

3.3. Simulation results of turbulent flow

In the turbulent flow case, the turbulent velocity profile obtained numerically with an average velocity of 1.0 m/s ($Re = 19{,}923$) is used. The standard k-ε model with standard wall function was applied in the simulations.

Fig. 7 plotted the profiles of velocity (V_x), electric field (E_z), current density (j_z) and electric potential (U) along the chord connecting the electrodes without taking the Lorentz force into account. In contrast to the laminar case, the broad velocity profile in the turbulent case generated broad profiles in the electric field and current density. This creates an almost linearly increasing electric potential profile along the chord connecting the electrodes. The difference in the electric potential on two electrodes was about 0.002 V and consistent with the theoretical value. This is confirmed in the contour plot of electric potential on the vertical cross section through the electrodes (Fig. 8). Compared to the

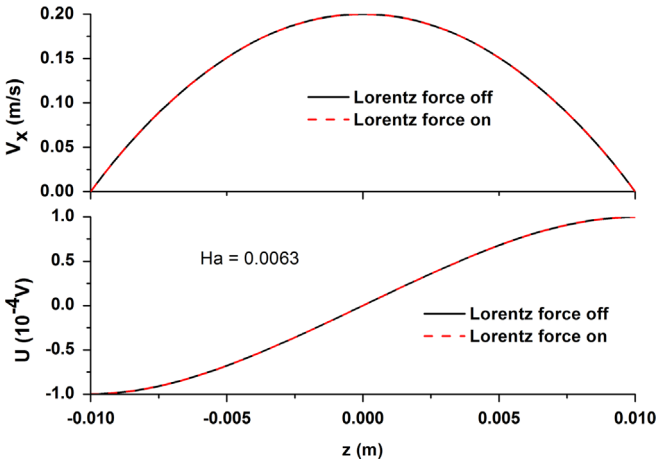

Fig. 6. The effect of Lorentz force on velocity profile and electric potential for laminar flow case.

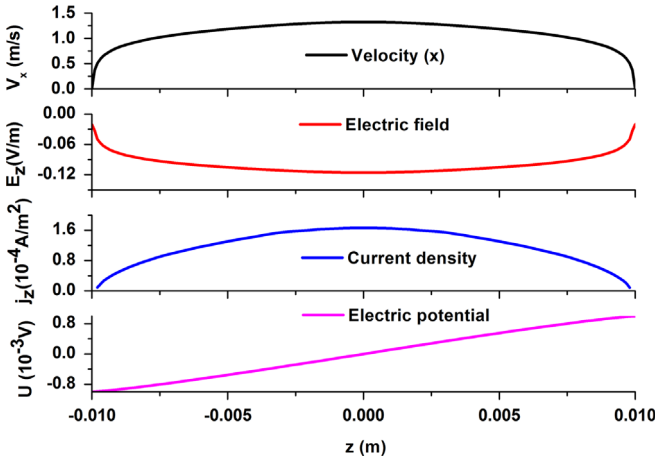

Fig. 7. Profiles of velocity, electric field, current density and electric potential along the chord connecting the electrodes for a turbulent flow.

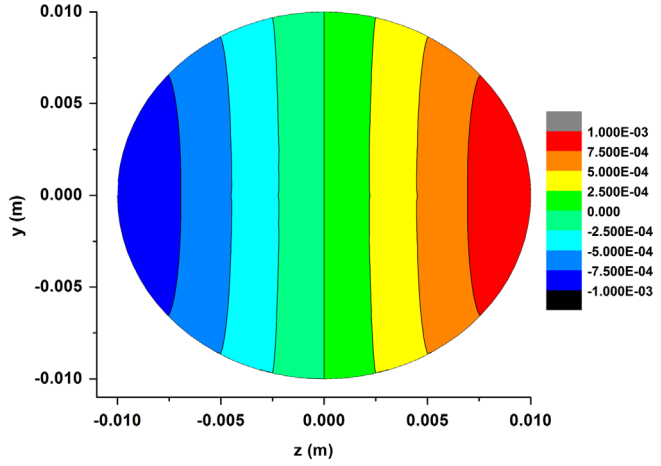

Fig. 8. Contour of electric potential in the vertical cross section of flowmeter pass the electrodes.

laminar flow case, the distribution of electric potential is more uniform and the lines with constant potentials were nearly parallel to the y axis in the center. The lines were much more bent in the laminar case.

The effect of Lorentz force was also checked. Since the Hartmann number is the same as the laminar flow case, its small magnitude

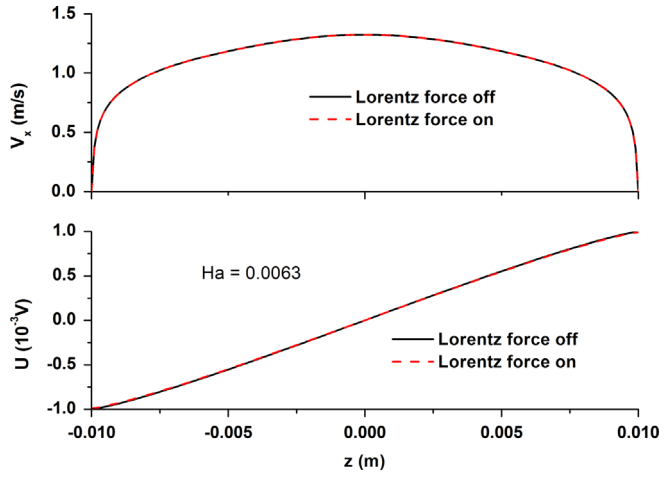

Fig. 9. The effect of Lorentz force on velocity profile and electric potential for the turbulent flow case.

should not change the velocity profile or electric potential when the Lorentz force is included in the momentum equation. Fig. 9 shows the velocity profile and electric potential are nearly constant with the Lorentz force included in the momentum equation.

Due to the small electric conductivity used in the current simulations, the electromagnetic force has no appreciable effect on the characteristics of the flowmeter. However, for liquid metals such as mercury and liquid sodium, the electric conductivity is as large as 10^6 S/m and the corresponding Hartmann number will be a few hundred, with other parameters the same as those used here [16]. In that case, the velocity profile will be largely determined by the induced electromagnetic force and not by the viscous force.

4. Conclusions

Numerical simulations were performed using integrated MHD/CFD simulations to study the characteristics of the electromagnetic flowmeter with point electrodes for both laminar and turbulent flows. Grid sensitivity and convergence studies were performed to assure the computational outcomes are accurate. Induced electric field and electric potential profiles were obtained directly thought the coupling of MHD equations in the simulations. It was found that the numerical results agree with values from simplified analysis. The contours of electric potentials are calculated using this approach, and turbulent flow was shown to have a more uniform potential distribution than the laminar flow. Induced Lorentz force was also examined and its effect on the output signal was determined to be negligible for cases of small electric conductivity or Hartmann number used in these simulations. While the influence of the fluid conductivity is not large in these cases, the low Hartmann number facilitated testing of the integrated MHD/CFD solution method against conventional weighting function analysis methods that only apply to low conductivity fluids, helping to validate the simulation approach.

References

[1] Shercliff JA. Relation between the velocity profile and the sensitivity of electromagnetic flowmeters. Journal of Applied Physics 1954;25:817–8.
[2] Shercliff JA. The theory of electromagnetic flow measurement. Cambridge University Press; 1954.
[3] Bevir MK. The theory of induced voltage electromagnetic flowmeters. Journal of Fluid Mechanics 1970;43:577–90.
[4] Bevir MK, O'Sullivan VT, Wyatt DG. Computation of electromagnetic flowmeter characteristics from magnetic field data. Journal of Physics D: Applied Physics 1981;14:373–88.
[5] Wyatt DG. Computation of electromagnetic flowmeter characteristics from magnetic field data. II. Errors. Journal of Physics D: Applied Physics 1983;16:465–78.
[6] O'Sullivan VT, Wyatt DG. Computation of electromagnetic flowmeter characteristics from magnetic field data: III. Rectilinear weight functions. Journal of Physics D: Applied Physics 1983;16:1461–76.
[7] Nashed M. Solution of the electromagnetic flowmeter equation. Journal of Physics: Applied Physics 1972;5:L33–66.
[8] Hemp J, Versteeg HK. Prediction of electromagnetic flowmeter characteristics. Journal of Physics D: Applied Physics 1986;19:1459–76.
[9] Luntta E, Halttunen J. The effect of velocity profile on electromagnetic flow measurement. Sensor and Actuators 1989;16:335–44.
[10] Zhang XZ, Hemp J. Calculation of the virtual current around an electromagnetic velocity probe using the alternating method of Schwarz. Flow Measurement and Instrumentation 1994;5(146):9.
[11] Lim KW, Chung MK. Relative errors in evaluation the electromagnetic flowmeter signal using the weight function method and the finite volume method. Flow Measurement and Instrumentation 1998;9:229–35.
[12] Lim KW, Chung MK. Numerical investigation on the installation effects of electromagnetic flowmeter downstream of a 90° elbow—laminar flow case. Flow Measurement and Instrumentation 1999;10:167–74.
[13] Wang JZ, Lucas GP, Tian GY. A numerical approach to the determination of electromagnetic flow meter weight functions. Measurement Science and Technology 2007;18:548–54.
[14] Wang JZ, Tian GY, Lucas GP. Relationship between velocity profile and distribution of induced potential for an electromagnetic flow meter 2007;18:99–105.
[15] Wang X, Yurii Kolenikov, Thess A. Numerical calibration of a Lorentz force flowmeter. Measurement Science and Technology 2012;23:045005.
[16] Zhou T, Yang Z, Ni M, Chen H. Code development and validation for analyzing liquid metal MHD flow in rectangular ducts. Fusion Engineering and Design 2010;85:1736–41.
[17] Wang PJ, Chang CY, Chang ML. Biosensors and Bioelectronics 2004;20:115–21.
[18] Moreau RJ. Magnetohydrodynamics (Fluids Mechanics and its Applications). Kluwer Academic Publishers; 1990.